ORIGINAL PAPER

Nagoya J. Med. Sci. **83**. 277–286, 2021
doi:10.18999/nagjms.83.2.277

Distribution of scatter radiation by C-arm cone-beam computed tomography in angiographic suite: measurement of doses and effectiveness of protection devices

Mayako Yamaji[1], Tsuneo Ishiguchi[1], Shuji Koyama[2], Shuji Ikeda[1], Akira Kitagawa[1], Makiyo Hagihara[1], Yuji Itoh[3], Masaru Nakamura[3], Toyohiro Ota[1] and Kojiro Suzuki[1]

[1]*Department of Radiology, Aichi Medical University, Nagakute, Japan*
[2]*Department of Radiological Technology, Nagoya University School of Health Sciences, Nagoya, Japan*
[3]*Department of Radiology, Aichi Medical University Hospital, Nagakute, Japan*

ABSTRACT

Distribution of radiation by C-arm cone-beam computed tomography (CBCT) in the angiographic suite and effectiveness of protection devices were assessed. CBCT image of a human phantom was obtained by a rotation of 220 degrees during 8 seconds of exposure. One hundred and twelve dosimeters were placed at different positions around the beam entry site, and color maps of dose distributions were drawn for horizontal and vertical planes. The measurements showed the highest radiation dose over 600 μGy by a single CBCT image acquisition at a distance of 60 cm from the beam entry site and a height of 90 cm from the floor. The color maps demonstrated the dose distribution to be more intense at the bilateral directions of the phantom. With the use of a ceiling-mounted transparent lead-acryl screen and a table-suspended lead curtain, the doses were reduced by 45–92 % at a direction of 210 degrees and a distance of 120 cm.

Keywords: scatter radiation, radiation protection, cone-beam computed tomography

Abbreviations:
CBCT: cone-beam computed tomography
DSA: digital subtraction angiography
OSL: optically stimulated luminescence
HCC: hepatocellular carcinoma
TACE: transarterial chemoembolization

INTRODUCTION

Cone-beam computed tomography (CBCT) is a technology that provides three-dimensional images by rotating the X-ray tube and flat-panel detector mounted on a C-arm of the angiographic equipment. CBCT has been used during various fluoroscopy-guided interventional radiologic procedures including arterial embolization, endovascular stent-graft deployment, percutaneous tumor ablation, biopsy and drainage. CBCT facilitates detection of lesions, understanding of

Received: June 4, 2020; accepted: October 28, 2020
Corresponding Author: Mayako Yamaji, MD
Department of Radiology, Aichi Medical University, 1-1 Yazako Karimata, Nagakute 480-1195, Japan
Tel: +81-561-63-1481; fax: +81-561-63-3268, E-mail: mayakom@aichi-med-u.ac.jp

the anatomy, navigation of devices and confirmation of the results of treatment.[1-3] CBCT-guided intervention has also been reported to lead to reductions in contrast doses, operative times and patient radiation exposure during the procedure compared with the conventional method using only fluoroscopy or digital subtraction angiography (DSA).[4,5]

On the other hand, a limited number of studies have reported on the amount and distribution of the scatter radiation that the operators and attending staff are exposed to during CBCT-guided interventional procedures.[6] The present study was undertaken to evaluate the dose and distribution of scatter radiation by CBCT in the angiographic suite and to assess the effectiveness of the protection devices used.

MATERIALS AND METHODS

A floor-mounted C-arm angiography equipment with a 38 cm × 30 cm flat panel detector (Axiom Artis dFA, Siemens, Erlangen, Germany) was used for the study. The phantom used for the experiment was an anthropomorphic phantom (Rando Phantom, The Phantom Laboratory, Salem, NY, USA), which is equivalent to the human body in terms of x-ray absorption and scattering (Figure 1a). Thickness of the abdomen of the phantom was 27 cm. The phantom was placed on the patient table, and CBCT images of the abdominal part of the phantom were obtained with a field-of-view of 24 cm × 18 cm by a rotation of 220 degrees during 8 seconds of exposure. The rotation of the C-arm started from the position with the x-ray tube on the left side of the phantom and, passing under the patient table, stopped when the tube came to the

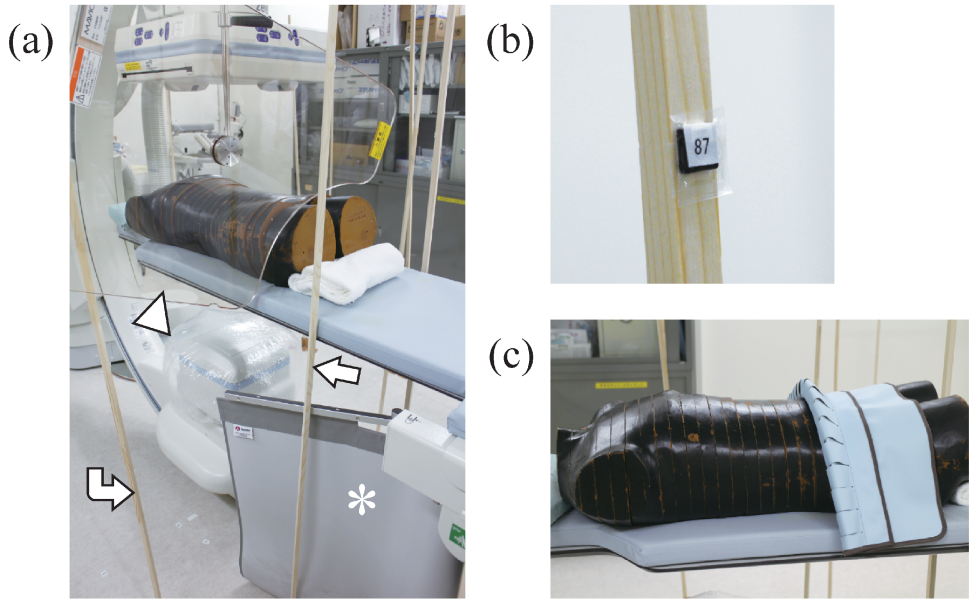

Fig. 1 Pictures of equipment

Fig. 1a: Picture showing the C-arm, an anthropomorphic phantom, a ceiling-mounted transparent lead-acryl screen (arrowhead) and a table-suspended lead curtain (asterisk). Arrow and curved arrow show a 210 degrees/60 cm rod and a 240 degrees/60 cm rod, respectively.

Fig. 1b: A nanoDot dosimeter attached to the wooden rod.

Fig. 1c: A lead-containing edged protective sheet placed on the lower abdomen of the phantom.

right side of the phantom. The tube voltage was set at 90 kV and the tube current was operated by automatic exposure control that provides the exposure needed to produce a predetermined image quality by sampling the x-ray intensity at the detector.

A dosimeter system using optically stimulated luminescence (OSL) with aluminum oxide (nanoDot, Landauer Corporate, Glenwood, IL, USA) was used for measurement of the scatter radiation.[7] Each dosimeter was 10 × 10 mm, and was attached to the wooden rods vertically placed on the floor (Figure 1b). One-hundred and twelve dosimeters were arranged at different heights, distances, and directions around the beam entry site. The positions of the dosimeters were as follows: height from the floor; 45, 90, 135 and 180 cm, distance from the beam entry site; 60, 120, 240 and 360 cm, horizontal direction; every 30 degrees around the phantom (Figure 2a, b). The dosimeters were placed so as not to lie in the way of the rotation of the C-arm or patient table. Thus, the dosimeters at the direction of 0 and 30 degrees were placed only at the 240 cm site and those of 180 degrees only at the 240 and 360 cm sites. As a reference, an ionization chamber dosimeter (9060/ 10X5-1800, Radcal, Monrovia, CA, USA) was placed at a height of 135 cm from the floor, a distance of 120 cm from the beam entry site and a direction of 240 degrees.

Scatter radiation was measured without and with protective devices including a ceiling-mounted transparent lead-acryl screen (Transparent acrylic shield OT25B050, 0.5 mm-lead equivalent, 60 cm wide × 76 cm high, Mavig, Munich, Germany) and a table-suspended lead curtain (Lower body x-ray shields, 312/DS-039/1, 0.5 mm-Pb equivalent, 118 cm wide × 75 cm high, Kenex, Essex, England) (Figure 1a), or a lead-containing edged protective sheet placed on the lower abdomen of the phantom (Edge Protector, Rikutoh, Tokyo, Japan)[8] (Figure 1c). The ceiling-

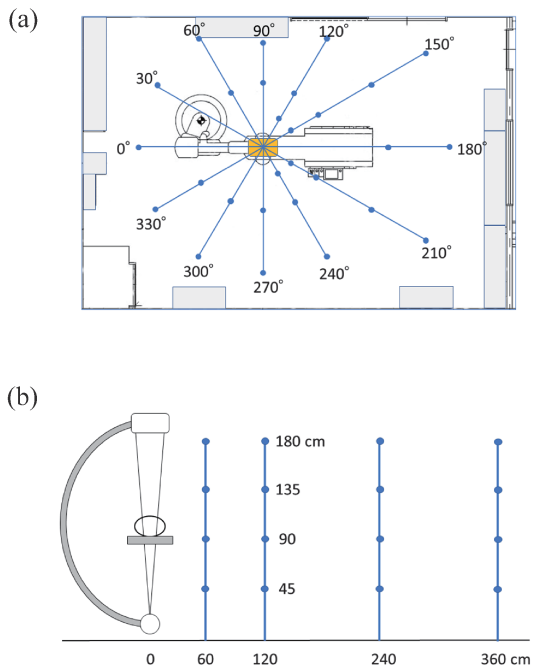

Fig. 2 Positions of dosimeters
Fig. 2a: Positions of dosimeters in horizontal plane.
Fig 2b: Positions of dosimeters in vertical plane.

mounted transparent lead-acryl screen was positioned at the inner side of the vertically placed rod of 210 degrees/60 cm and at the external side of the vertically placed rod of 240 degrees/60 cm. The table-suspended lead curtain was positioned at the inner side of the vertically placed rod of 210 degrees/60 cm (Figure 1a). CBCT image acquisition was repeated 20 times, and 1/20 of the readout of each dosimeter was regarded as the mean dose by a single CBCT image acquisition.

The following equation was used to estimate the scatter radiation doses of evaluation points:

$$Da = \frac{Db \times b^2}{a^2}$$

where Da is an estimated dose of evaluation point A; Db is a measured dose of measuring point B; a and b are the distances from the beam center to point A and point B placed on the relevant line, respectively. These points were set at distance intervals of 20 cm at each of the heights of 45, 90, 135 and 180 cm and every 30 degrees around the phantom. The distance from the beam center to base of the patient table was 80 cm on the line of 180 degrees. Thus, the doses within 80 cm at a direction of 180 degrees were substituted by the average dose of 150 and 210 degrees. As to the doses within 60 cm at a direction of 210 degrees with protection devices, the estimated doses above the equation could not be used. Thus, the estimated doses without protection devices were substituted in this area. All calculations were performed by using spreadsheet software (Microsoft Excel 2013, Microsoft Japan, Tokyo). Color maps of dose distributions in the angiographic suite were drawn for each horizontal and vertical plane by using graphing software (Griview3D, Graduate School of Science, Osaka City University, Osaka, Japan).

RESULTS

Correlation of the readout values of the OSL dosimeters and the ion chamber dosimeter are shown in Table 1. Measured doses by the OSL were 17–41 % higher than those by the ion chamber dosimeter.

Table 2 shows measured and estimated doses of 180, 210, and 240 degrees without and with protection devices. And Figure 3 presents the color maps in the horizontal plane at the height of 45 cm, 90 cm, 135 cm and 180 cm. Measurements showed the highest radiation dose exceeding 600 μGy by a single CBCT image acquisition at a distance of 60 cm from the beam entry site and a height of 90 cm from the floor (818.7 μGy at a direction of 120 degrees, 669.6 μGy at a direction of 240 degrees). The color maps demonstrated that the doses were more intensively distributed in bilateral directions of the phantom, and they diminished with increasing distance from the beam entry site in accordance with the inverse square law.

Figure 4 shows the color map of vertical plane in the direction of 210 degrees without a protection device, representing the typical position of the interventional radiologist during angiographic procedures.

With the use of a ceiling-mounted lead-acryl screen and a table-suspended lead curtain, the doses reduced within the area of coverage (Figure 5). And the dose reduction rates were 45–92 % at a direction of 210 degrees and a distance of 120 cm (Table 2).

With the use of a lead-containing edged protective sheet placed on the phantom and with the table-suspended lead curtain, the doses reduced at the caudal directions of the phantom (Figure 6). And the dose reduction rates were 32–60 % at a direction of 210 degrees and a distance of 120 cm (Table 2).

Table 1 Correlation of the readout values of the OSL dosimeters and ion chamber dosimeter

	Without protection device	Ceiling-mounted lead-acryl screen + Table-suspended lead curtain	Edged protective sheet + Table- suspended lead curtain
Ion chamber dosimeter	113.5 μGy	8.1 μGy	88.5 μGy
OSL dosimeter	150.0 μGy	9.5 μGy	124.5 μGy
OSL/ ion chamber	132 %	117 %	141 %

OSL: optically stimulated luminescence

Table 2 Measured and estimated doses of 180, 210, and 240 degrees without and with protection devices

	Direction		
	180 degrees	210 degrees	240 degrees
Distance/Height	A/B/C (μGy)	A/B/C (μGy)	A/B/C (μGy)
60 cm/45 cm	377.0*/377.0*/377.0*	372.9/21.9/20.2	357.0/344.8/343.7
/90 cm	304.0*/304.0*/304.0*	288.6/258.0/272.0	669.6/685.4/636.9
/135 cm	188.8*/153.6*/172.8*	269.6/12.3/117.6	455.2/519.7/413.7
/180 cm	304.0*/176.0*/193.6*	209.6/183.3/160.7	214.1/222.2/206.1
120 cm/45 cm	5.6*/5.6*/4.4*	101.8/51.1/47.1	143.6/141.1/132.5
/90 cm	3.2*/3.6*/3.6*	77.8/42.6/43.0	164.4/143.5/143.6
/135 cm	47.2*/38.4*/43.2*	97.0/18.3/38.7	150.0/9.5/124.5
/180 cm	76.0*/44.0*/48.4*	89.9/7.5 /61.3	118.4/8.8 /93.2
240 cm/45 cm	1.4/1.4/1.1	21.5/17.9 /15.0	32.7/32.9 /30.4
/90 cm	0.8/0.9/0.9	20.4/7.8/8.6	37.6/25.6/31.9
/135 cm	11.8/9.6/10.8	22.5/6.9/10.1	38.6/8.3/31.6
/180 cm	19.0/11.0/12.1	23.9/6.3/14.3	34.1/8.5/30.4

* An estimated dose

A: Measured dose without a protection device.

B: Measured dose with the use of a ceiling-mounted lead-acryl screen and a table-suspended lead curtain.

C: Measured dose with the use of a lead-containing edged protective sheet and a table-suspended lead curtain.

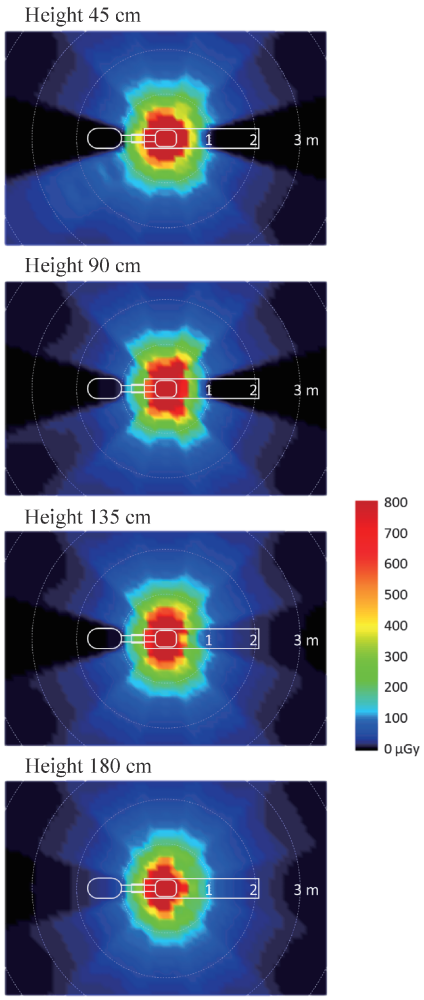

Fig. 3 Color maps of distribution of scatter radiation at horizontal planes Dose distribution is more intense at bilateral directions of the phantom at every height.

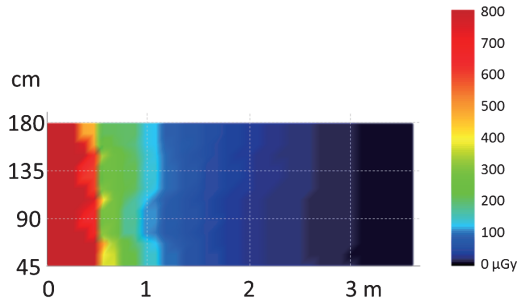

Fig. 4 Color map at vertical plane at a direction of 210 degrees

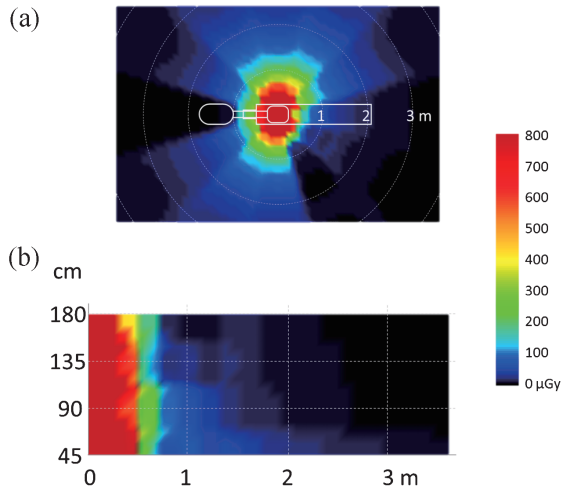

Fig. 5 Color maps of distribution of scatter radiation with the ceiling-mounted screen and table-suspended curtain
Fig. 5a: Color map of horizontal plane at the height of 135 cm.
Fig. 5b: Color map of vertical plane in the direction of 210 degrees.

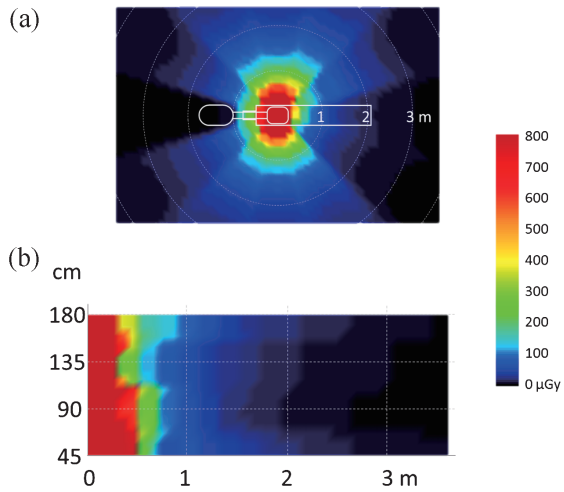

Fig. 6 Color maps of distribution of scatter radiation with the edged protective sheet and table-suspended curtain
Fig 6a: Color map of horizontal plane at the height of 135 cm.
Fig 6b: Color map of vertical plane in the direction of 210 degrees.

DISCUSSION

The clinical advantages of CBCT-guided interventional procedures have been widely reported. Dijkstra et al reported that CBCT utilizing fusion imaging was valuable in complicated endovascular aortic aneurysm repair with reduction of the volume of contrast material needed, and

post-procedure CBCT was useful to evaluate successful aneurysm exclusion and detect early complications.[4] Kothary et al showed that radiation exposure to patients and the dose of iodinated contrast medium during transarterial chemoembolization (TACE) for hepatocellular carcinoma (HCC) were reduced by use of CBCT.[6] Miyayama et al showed that CBCT-arteriography based TACE guidance software is sufficient to identify small HCCs and their feeding branches to facilitate successful treatment.[9] Their published results also documented that intraprocedural CBCT monitoring reduced the rate of local tumor recurrence.[3] For non-vascular interventional procedures, Mckay et al reported that procedure times for percutaneous abscess drainage using CBCT-based needle guidance were significantly shorter than when using conventional CT guidance with similar success rates.[10]

With the widening application of CBCT technology, there has been increasing awareness of the importance of radiation exposure to interventional radiologists and other staff members. Schulz et al evaluated the radiation exposure for operating personnel associated with CBCT and demonstrated that CBCT angiography significantly increased radiation exposure to the attending operator in comparison with two dimensional angiography. They recommended that the physician wear protective devices and leave the examination room when performing CBCT.[6] In the clinical settings of CBCT, however, there are cases that require the continuing presence in the room of the physicians or staff for reasons such as watching and supporting an unstable patient or performing rotational angiography via a small vessel under manual contrast injection from a microcatheter. Under these circumstances, it is important to know the distribution of scatter radiation by CBCT, to use protective tools effectively and to stand at a position with a lower radiation dose.

OSL dosimeters have been widely used to monitor occupational radiation doses for the staff of radiology departments in many hospitals.[11] The dosimeter used in this study, nanoDot, is small, easy to handle and suitable for dose measurements at multiple positions. It has a wide operating energy range (5 keV–20 MeV) with accuracy within ±10 % over the diagnostic energy range (70–140 kVp), minimal angular dependence and useful dose range of 10 μGy to >100 Gy with linear response with dose up to 300 cGy.[7] The readout values of nanoDot were 17–41 % higher in comparison with the ion-chamber dosimeter that was used as the standard reference. Even though this potential overestimation might be included in a critical evaluation, overall measurement by nanoDot was considered to be stable and reliable.

The present study showed the highest radiation dose of 600–800 μGy by a single CBCT image acquisition to be at a distance of 60 cm from the beam entry site. In 2012, the International Commission on Radiological Protection (ICRP) lowered the threshold dose of lens opacity, and recommended for occupational exposure an equivalent dose limit for the lens of the eye of 20 mSv in a year, averaged over defined periods of 5 years.[12] Our result indicates that, if CBCT was performed with a physician standing near the beam entry site without a protective device, the dose limit for the lens of the eye would be reached by the time at which approximately 30 CBCT image acquisitions were performed. Though this may be an overstated assumption, it serves to highlight the fact that optimal use of protective devices is mandatory for physicians or other staff remaining in the room for any reason.

The scatter radiation distributed more intensively in the bilateral directions of the phantom (Figure 3). If a physician or staff member needs to observe the patient near the table, it would be recommended to stand in the back of the base of C arm. With the use of a ceiling-mounted transparent lead-acryl screen and a table-suspended lead curtain, the doses were reduced 45–92 % at a direction of 210 degrees and a distance of 120 cm (Table 2). If a physician needs to stand beside the table and inject contrast material manually, for example, during CBCT acquisition, it would be recommended to place the ceiling-mounted lead-acryl screen and the table-suspended

lead curtain exactly between the beam entry site and the personnel. It should be noted that the protective devices effectively shield the scatter radiation only in a limited direction (Figure 5). Our data are consistent with the phantom study by Schulz et al that reported that ceiling-mounted glass shield, with a lead equivalent value of 0.5 mm placed in front at the face level with a gap of 35 cm, attenuated 86.7 % of the radiation to the eye.[6] It is estimated that, when the highest radiation dose of 600–800 μGy by a single CBCT image acquisition is reduced by 80 % with use of these protective devices, more than 120 image acquisitions could be performed acceptably before the eye dose would reach the limit of 20 mSv in a year. Floor-standing movable transparent lead-acryl screen will provide additional shielding capability for other personnel. Use of protective eyewear or safety glasses is always recommended.

Another protective device used in this study, Edge Protector, was originally designed for reduction of scatter radiation to the physician during CT-fluoroscopy guided interventions.[8] The lead-containing edge of the protective sheet attenuated scatter radiation by CBCT toward the caudal direction (Figure 6). Placement of the Edge Protector on the lower abdomen of the phantom did not apparently influence the image of CBCT.

Our results showed that, in combination with a table-suspended curtain, a ceiling-mounted screen was more effective in shielding scatter radiation than Edge Protector. We consider that a ceiling-mounted screen and a table-suspended curtain should be routinely used for vascular interventional procedures, while Edge Protector might be used instead of a screen for procedures requiring percutaneous puncture including needle biopsy, abscess drainage or thermal ablation. We would also recommended that any personnel watching the patient during CBCT image acquisition stand behind the base column of the floor-mounted C-arm where scatter radiation was the least in every situation.

The present study has some limitations. First, the number of dosimeters was low. The nearest measuring points from the beam center were 60cm in distance and those at a direction of 0, 30, and 180 degrees were 240 cm. The dose distributions within the measuring points were evaluated by estimation doses. Thus, numerous estimation doses were used to make color maps of dose distributions. Second, only one anthropomorphic phantom was used for the experiment. In clinical situations, scatter radiation from a larger patient would be more associated with the increase of x-ray output. Last, only two combinations of protective devices were evaluated in the present study. Further study with combinations of other devices will also be needed.

In conclusion, interventional radiologists and other staff should be aware of the dose levels of scatter radiation by CBCT and its characteristic distribution. Use of protective devices including ceiling-mounted lead-acryl screen, table-suspended lead curtain and lead-containing edged protective sheet are effective in reducing the dose in a particular direction.

CONFLICT OF INTEREST

The authors have no conflict of interest to declare.

REFERENCES

1 Abi-Jaoudeh N, Kruecker J, Kadoury S, et al. Multimodality image fusion guided procedures: technique, accuracy, and applications. *Cardiovasc Intervent Radiol*. 2012;35(5):986–998. doi:10.1007/s00270-012-0446-5.
2 Angle JF. Cone-beam CT: vascular applications. *Tech Vasc Interv Radiol*. 2013;16(3):144–149. doi:10.1053/j.tvir.2013.02.009.
3 Miyayama S, Yamashiro M, Hashimoto M, et al. Comparison of local control in transcatheter arterial

chemoembolization of hepatocellular carcinoma ≤6 cm with or without intraprocedural monitoring of the embolized area using cone-beam computed tomography. *Cardiovasc Intervent Radiol*. 2014;37(2):388–395. doi:10.1007/s00270-013-0667-2.

4 Dijkstra ML, Eagleton MJ, Greenberg RK, Mastracci T, Hernandez A. Intraoperative C-arm cone-beam computed tomography in fenestrated/branched aortic endografting. *J Vasc Surg*. 2011;53(3):583–590. doi:10.1016/j.jvs.2010.09.039.

5 Kothary N, Abdelmaksoud MHK, Tognolini A, et al. Imaging guidance with C-arm CT: prospective evaluation of its impact on patient radiation exposure during transhepatic arterial chemoembolization. *J Vasc Interv Radiol*. 2011;22(11):1535–1543. doi:10.1016/j.jvir.2011.07.008.

6 Schulz B, Heidenreich R, Heidenreich M, et al. Radiation exposure to operating staff during rotational flat-panel angiography and C-arm cone beam computed tomography (CT) applications. *Eur J Radiol*. 2012;81(12):4138–4142. doi:10.1016/j.ejrad.2012.01.010.

7 LANDAUER. nanoDot dosimeter. http://www.landauer.com/product/nanodot. Accessed December 15, 2019.

8 RIKUTOH. Edge protector [in Japanese]. http://rikutoh.com/products/needle. Accessed December 15, 2019.

9 Miyayama S, Yamashiro M, Hashimoto M, et al. Identification of small hepatocellular carcinoma and tumor-feeding branches with cone-beam CT guidance technology during transcatheter arterial chemoembolization. *J Vasc Interv Radiol*. 2013;24(4):501–508. doi:10.1016/j.jvir.2012.12.022.

10 McKay T, Ingraham CR, Johnson GE, Kogut MJ, Vaidya S, Padia SA. Cone-beam CT with fluoroscopic overlay versus conventional CT guidance for percutaneous abdominopelvic abscess drain placement. *J Vasc Interv Radiol*. 2016;27(1):52–57. doi:10.1016/j.jvir.2015.09.016.

11 Yukihara EG, McKeever SWS. Optically stimulated luminescence (OSL) dosimetry in medicine. *Phys Med Biol*. 2008;53(20):R351–R379. doi:10.1088/0031-9155/53/20/R01.

12 Authors on behalf of ICRP;Stewart FA, Akleyev AV, Hauer-Jensen M, et al. ICRP publication 118: ICRP statement on tissue reactions and early and late effects of radiation in normal tissues and organs--threshold doses for tissue reactions in a radiation protection context. *Ann ICRP*. 2012;41(1-2):1–322. doi:10.1016/j.icrp.2012.02.001.